HHS Public Access

Author manuscript

J Pathol. Author manuscript; available in PMC 2016 August 01.

Published in final edited form as:

J Pathol. 2015 August ; 236(4): 421–432. doi:10.1002/path.4538.

Loss of Tumour Suppressor PTEN Expression in Renal Injury Initiates SMAD3 and p53 Dependent Fibrotic Responses

Rohan Samarakoon[1], **Sevann Helo**[2], **Amy D Dobberfuhl**[2], **Nidah S Khakoo**[1], **Lucas Falke**[3], **Jessica M Overstreet**[1], **Roel Goldschmeding**[3], and **Paul J Higgins**[1]

[1]Center for Cell Biology and Cancer Research, Albany Medical Center, 47 New Scotland Avenue, Albany, NY 12208 [2]Division of Urology, Albany Medical Center, 47 New Scotland Avenue, Albany, NY 12208 [3]Department of Pathology, University Medical Center Utrecht, The Netherlands

Abstract

Deregulation of the tumour suppressor PTEN occurs in lung and skin fibrosis, diabetic and ischaemic renal injury. However, the potential role of PTEN and associated mechanisms in the progression of kidney fibrosis is unknown. Tubular and interstitial PTEN expression was dramatically decreased in several models of renal injury including aristolochic acid nephropathy (AAN), streptozotocin (STZ)-mediated injury and ureteral unilateral obstruction (UUO), correlating with Akt, p53 and SMAD3 activation and fibrosis. Stable silencing of PTEN in HK-2 human tubular epithelial cells induced dedifferentiation and CTGF, PAI-1, vimentin, α-SMA and fibronectin expression compared to HK-2 cells expressing control shRNA. Furthermore, PTEN knockdown stimulated Akt, SMAD3 and $p53^{Ser15}$ phosphorylation with an accompanying decrease in population density and an increase in epithelial G_1 cell cycle arrest. SMAD3 or p53 gene silencing or pharmacological blockade partially suppressed fibrotic gene expression and relieved growth inhibition orchestrated by deficiency or inhibition of PTEN. Similarly, shRNA suppression of PAI-1 rescued the PTEN loss-associated epithelial proliferative arrest. Moreover, TGF-β1-initiated fibrotic gene expression is further enhanced by PTEN depletion. Combined TGF-β1 treatment and PTEN silencing potentiated epithelial cell death via p53 dependent pathways. Thus, PTEN loss initiates tubular dysfunction via SMAD3- and p53-mediated fibrotic gene induction with accompanying PAI-1 dependent proliferative arrest, and cooperates with TGF-β1 to induce the expression of profibrotic genes and tubular apoptosis.

Keywords

PTEN; SMAD3; p53; Akt; PAI-1; CTGF; UUO; AAN; Renal Fibrosis

Correspondence: Dr. Rohan Samarakoon or Dr. Paul J. Higgins, Center for Cell Biology & Cancer Research (MC-165), Albany Medical College, 47 New Scotland Avenue, Albany, New York 12208, Tel: 518-262-5168, samarar@mail.amc.edu or higginp@mail.amc.edu.

Disclosure: The authors have no conflict of interest.

Author Contributions:

RS and PJH conceived and designed the experiments; RS, SH, LF, ADD and JMO and performed the experiments and all were involved in data analysis; RG contributed key reagents/materials/analysis tools; RS and PJH wrote the paper and all authors agreed on the manuscript prior to submission.

Introduction

Chronic kidney disease (CKD), estimated to affect 8–16% of the world population, has become a major public health burden largely due to the continued increase in diabetes, hypertension and other risk factors such as acute or toxic-renal injury (1–3). Renal fibrosis is marked by tubular injury/epithelial growth arrest/death, interstitial expansion, persistent inflammation and excess deposition of extracellular matrix (ECM) proteins leading to nephron loss and chronic renal insufficiency (4–6). While TGF-β1 and angiotensin II are widely regarded as key orchestrators of kidney fibrosis regardless of initial insult (7,8), effective treatment to halt the progression of CKD and organ failure is largely lacking (9). Thus, identification of novel fibrotic factors and their cross-talk with established mediators of renal disease progression is of critical importance.

Phosphate Tensin Homologue on Chomosome 10 (PTEN), the principle negative regulator of the PI3K pathway and Akt activation is a tumour suppressor that is lost or mutated in various malignancies (10,11). Recent studies suggest a role for PTEN in the progression of tissue fibrosis. PTEN deficiency is characteristic of idiopathic pulmonary fibrosis (IPF) and genetic ablation of PTEN in the alveolar epithelium promotes lung fibrosis via Akt activation and increased epithelial dedifferentiation/ plasticity (12,13), a phenotype that is associated with cancer progression and organ fibrosis (14). Similarly, PTEN loss in dermal fibroblasts is sufficient to drive skin fibrosis and increase myofibroblast activation in mice (15). Attenuation of PTEN expression is also evident in glomeruli of the diabetic kidney promoting glomerular hypertrophy via Akt dependent pathways (16). In the setting of ischaemic renal injury, tubular PTEN down-regulation correlated with epithelial dedifferentiation (17). Glucose, moreover, decreased PTEN expression in mesengial cells (18). Definition of molecular pathways downstream of PTEN consequent to renal injury may not only provide a rationale for context-dependent phenotypic effects but also lead to the identification of novel targets to suppress the aberrant tissue repair response associated with PTEN dysregulation. Underscoring this approach is the fact that currently there are no pharmacological tools to rescue PTEN expression as an “anti-fibrotic” therapy.

TGF-β1 is an established inducer of genes encoding fibrotic effectors, the most prominent of which are PAI-1, CTGF, collagen-1 and fibronectin (19–22). TGF-β1 also mediates epithelial cell cycle arrest, apoptosis and the progression of acute kidney injury to fibrosis (23,24). Tumour suppressor p53, a master regulator of cell cycle arrest and death, regulates ischaemic-, obstructive- and aristolochic acid-induced kidney injury and disease progression (24–26). Furthermore, our recent studies established molecular interactions between p53 and SMAD2/3 transcription factors in orchestrating fibrotic renal responses (27,28). The mechanistic link between p53 and PTEN in promoting a fibrotic phenotype in the context of kidney injury, however, has not been explored. Furthermore, potential involvement of TGF-β1/SMAD2/3 downstream of PTEN, particularly in the context of tubulo-interstitial injury repair response is not clear.

This paper reports PTEN loss in both tubular and interstitial regions of UUO-, AAN- and STZ-injured kidneys. PTEN deficiency or inactivation in HK-2 human tubular epithelial cells also promotes epithelial dysfunction (fibrotic gene induction, epithelial cell cycle

arrest, dedifferentiation) mediated by SMAD3-, p53- and Akt-dependent pathways. Furthermore, PTEN knockdown or pharmacological inhibition also potentiates TGF-β1 initiated fibrotic gene changes as well as cell death.

Materials and Methods

Cell Culture and Reagents

Provided as Supplementary data.

Creation of Stable Cell Lines

HK-2 cells grown to 60–70% confluence in 10% FBS/DMEM were infected with PTEN or control shRNA lentiviral particles (Santa Cruz Biotechnology) in 5 μg/ml Polybrene +10%FBS/DMEM overnight. Following a 24 hour recovery period in complete media, cells stably expressing PTEN or control shRNA were split (1:3) in complete media containing Puromycin (5 μg/ml) and medium changed every 3 days. PTEN silencing was confirmed by western analysis. To generate HK-2 cultures with SMAD3, p53 or PAI-1 knock-down on a PTEN-depleted background, PTEN shRNA stable cells (at 60–70% population density) were re-infected with control or SMAD3, p53 or PAI-1 or control shRNA lentiviral constructs (Santa Cruz) as described above. p53, SMAD3 and PTEN double gene silencing was confirmed by immuno-blot analysis. To generate proximal tubular epithelial cells with PTEN overexpression, confluent HK-2 cells were infected with PTEN human ORF cDNA or control Lentifect lentiviral particles (GeneCopoeia) as above followed by a one day recovery period in complete media. Stable PTEN overexpressing cells were selected with Puromycin (5 μg/ml)+10%FBS/DMEM. Clones with modest PTEN overexpression were used for our experiments.

Unilateral Ureteral Ligation (UUO) in Mice

UUO and sham operations (in C57Bl/6 mice) were approved by the Experimental Animal Ethics Committee of the University of Utrecht. Briefly, mice were anaesthetized (by isoflurane inhalation) and a small incision made in the flank under aseptic conditions; the left ureter was exposed and ligated with two 5-0 silk sutures. Controls included sham-operated and the contralateral kidneys. Animals were euthanized 14 days postoperatively.

Aristolochic Acid-Induced Nephropathy (AAN) in Mice

As described previously (29), C57Bl/6 male mice received an intraperitoneal injection of aristolochic acid sodium salt (5 mg/kg body weight dissolved in distilled water; Sigma-Aldrich) once a day for 5 consecutive days or NaCl vehicle (control animals) alone. Both groups were sacrificed 25 days after the initial injection by ketamine–xylazine–atropine. An enzymatic assay (J2L Elitech, LabartheInard, France) was used for assessments of urinary creatinine levels in mice to confirm renal injury. The experimental Animal Ethics Committee of the University of Utrecht approved all AAN protocols.

Streptozotocin (STZ) Model of Renal Injury in Mice

This procedure was described previously (29) and performed with the approval of the Experimental Animal Ethics Committee of the University of Utrecht. C57Bl/6 mice (which included both male and female) were given a single intraperitoneal injection of 200 mg/kg streptozotocin (STZ; 30 mg/ml dissolved in 100 mM sodium citrate buffer, pH 4.5) (Sigma-Aldrich). Animals injected with sodium citrate buffer alone served as controls. Hyperglycaemia was determined 3 days after injection by measurement of blood glucose levels (Medisense Precision Xtra; Abbott, Bedford, IN). Non-responders were injected with a second dose of STZ. Animals had the continuous access to standard laboratory chow with daily addition of mash food. Prior to the induction of diabetes average blood glucose levels were at 8 mmol/L and 3 days after STZ injection average blood glucose levels rose to >20mmol/L. Slow release insulin pellets (Linshin, Scarborough, Canada) were implanted to animals 5 days after STZ injection. Blood was collected by cheek puncture for glucose measurement at 1, 3, and 6 months. Mice were sacrificed 26 weeks after induction of diabetes.

qRT-PCR Analysis

Total RNA was isolated from the renal cortex using TRIzol extraction reagent (Life technologies, Carlsbad, USA). μg of RNA was reverse transcribed to cDNA using standard procedures. Expression of target genes was determined using commercially available pre-designed TaqMan probes (Pten, Mm00477208_m1; Tbp, Mm00446971_m1; Life technologies, Carlsbad, USA). Samples were run on the Lightcycler 480 (Roche, Basel, Switzerland) and relative expression was determined using the ΔΔCT method. GeNorm determined the TATA box binding protein (TBP) to be the most stable reference gene in our experiment setup.

PAI-1 Promoter (Luciferase Reporter) Analysis

This procedure was performed as described previously (27,28).

Immunoblotting

Details in Supplementary Methods.

Co-Immunoprecipitation

Described in Supplementary Methods.

Immunohistochemistry

Detailed in Supplementary Methods.

Morphometric analysis

This procedure is detailed in the Supplementary Methods.

Cell cycle analysis

Control shRNA and PTEN shRNA expressing HK-2 cells were grown in serum containing media supplemented with Puromycin for 2–3 days. Following harvest with trypsin, cells

were incubated with soybean trypsin inhibitor, washed twice in PBS and fixed in 95% ethanol for 1 hour. Cultures were washed in PBS twice, incubated with RNaseA (20 μl/ml) and propidium iodide (2.5 μg/ml) in PBS/Triton-X 100 for 2 hours in the dark. Cell cycle distributions were measured using a FACS Calibur flow cytometer (Becton Dickinson, Franklin Lakes, NJ, USA) and analyzed with FlowJo software.

Statistical Analysis

Statistical differences were evaluated using ANOVA with Tukey post-hoc analysis and two-tailed Student's t-test. A p value of <0.05 considered significant and P values of <0.05, <0.01 or <0.001 are presented in individual histograms as asterisks, double asterisks and triple asterisks, respectively.

Results

Loss of PTEN expression in several models of renal injury and fibrosis

We utilized UUO-, AAN- and STZ-mediated renal damage as mouse models to investigate potential involvement of PTEN in the progression of renal injury and fibrosis. UUO is a widely used mouse model to mimic obstructive uropathy, which is a common cause of CKD in children (30). AAN is a form of renal failure due to consumption of herbals containing aristolochic acid (AA) in China (31). STZ-treatment in mice leads to diabetic nephropathy, which accounts for nearly 50% of CKD cases in the US (1–3).

Western blot analysis of the sham (Sham), contralateral (Contra) and obstructed mouse (UUO; day 14) kidneys revealed a dramatic loss in PTEN expression (Fig. 1A&B; $P<0.01$ vs contra or sham) while PAI-1 (Fig. 1A&C; $P<0.01$ vs contra or sham), pSMAD3 (Fig. 1A&D; $p<0.01$ vs contra or sham), α-SMA (Fig. 1A&E; $P<0.01$ vs contra or sham) and p-p53^{Ser15} (Fig. 1A&F; $P<0.01$ vs contra or sham) levels were dramatically increased in the ligated kidney relative to the sham or contralateral controls consistent with the loss of PTEN expression in renal fibrosis. Immunostaining using two specific antibodies against PTEN [rabbit-anti PTEN antibody (Fig. S1A&B; $P<0.001$)] and [mouse anti-PTEN antibody (Fig. S1C&D; $P<0.001$)] further confirmed a decrease in immunoreactive PTEN while pAKT (Fig. S1E) and total p53 levels (Fig. S1F&G; $P<0.001$) are increased in the fibrotic kidney in both the tubular and interstitial regions compared to contralateral counterparts. Interestingly, PTEN mRNA abundance between contralateral and UUO kidneys remained statistically insignificant, suggesting that PTEN loss is likely to occur at post-transcriptional/translational levels (Fig. S1H).

In AA- and STZ-treated mice, there is also a dramatic decline (90% and 70%, respectively) in PTEN levels in the tubulo-interstitial region relative to vehicle-treated control kidneys, which are NaCl for the AAN model (Fig. 2A&B; $P<0.001$) and sodium citrate for the STZ model (Fig. 2C&D; $P<0.001$). Loss of PTEN expression, moreover, correlated with increased expression of fibrosis marker fibronectin in both injury models (Fig. 2E for AAN and Fig. 2F for STZ), suggestive of a broader role for PTEN deregulation in renal tissue injury and maladaptive repair.

Targeted knockdown or inhibition of PTEN in HK-2 renal epithelial cells promotes cell cycle arrest, dedifferentiation and profibrotic gene expression

Stable gene silencing was utilized to investigate the phenotypic consequences of PTEN loss in HK-2 tubular epithelial cells and to mimic the loss of PTEN expression in damaged renal tubules in several kidney injury models (Figs. 1–2 & Fig. S1). PTEN gene depletion resulted in pAkt activation as expected while total Akt levels were unaffected (Fig. 3A). There is a substantial decrease (>37%; p <0.01) in population density in HK-2 cells with PTEN stable silencing compared to control shRNA-expressing cultures at day 3–5 (Fig. 3B&C). Flow cytometry reflected an accompanying increase in G1 and a decline in S phases of the cell cycle in PTEN shRNA transductants relative to control shRNA-expressing cells, suggesting a role for PTEN in epithelial cell growth arrest (Fig. 3D). PTEN depletion in HK-2 cultures also promotes a 4-fold increase (black bars; P<0.001) in cells with an elongated morphology with a parallel decrease in the cuboidal phenotype (grey bars; P<0.001) compared to the control shRNA population (Fig. 3E). PTEN shRNA expressing HK-2 cultures maintained in low serum (0.1% FBS) for 3–5 days upregulated CTGF (Fig. 3F&G; 12-fold; P<0.01), PAI-1 (Fig. 3F&H; 4-fold; P<0.05), fibronectin (Fig 3F&I; p <0.05), α-SMA, vimentin, p21 and TGF-β1 receptor II (RII) (Fig. 3F) expression compared to control shRNA cultures, confirming a role for PTEN deficiency in the induction of fibrotic genes and epithelial dedifferentiation. Similarly, inhibition of PTEN with VO induced an elongated morphology and a reduction in cell number ((Fig. 3J&K) compared to DMSO treated control cultures, which retained epithelial morphology. VO treatment, indeed, promotes AKT phosphorylation, consistent with PTEN inactivation (Fig. 3L). Preincubation of HK-2 cells with the Akt inhibitor, MK-2206 prior to VO stimulation not only suppressed pAKT activation (Fig. 3L) but also eliminated the VO-mediated decrease in cell number and induction of fibroblast morphology (Fig. 3J&K), suggestive of Akt function downstream of PTEN in modulating phenotypic changes.

SMAD3 activation downstream of PTEN absence promotes epithelial dysfunction

Given the involvement of the SMAD pathway in mediating growth suppressive effects in cancer (23) and renal fibrotic properties in response to TGF-β1 and angiotensin II (4–9,21), the role of SMAD3 downstream of PTEN loss was evaluated with regard to fibrosis marker expression, epithelial dedifferentiation and proliferative arrest. Stable silencing of PTEN in HK-2 cells, indeed, promoted a >5-fold increase in SMAD3 phosphorylation compared to mock transduced cultures (con shRNA) (Fig. 4A&B; P<0.01). To evaluate the SMAD3 pathway downstream of PTEN loss, cells with PTEN stable silencing were re-infected with SMAD3 shRNA [i.e., (PTEN+SMAD3) shRNA] or control shRNA [termed (PTEN+con) shRNA] lentiviral vectors (Fig. 4C). Expression of fibronectin, vimentin and PAI-1 (Fig. 4C&D), readily evident in (PTEN+con) shRNA cultures, are significantly diminished in dual PTEN and SMAD3 depleted cells [PTEN+SMAD3) shRNA] (Fig 4C), suggestive of SMAD3 effector function downstream of PTEN in orchestrating fibrotic gene changes. Elongated morphology evident in (PTEN+Con) shRNA HK-2 cells is also significantly decreased (>65%) in PTEN+SMAD3 knockdown cells (Fig. 4E; P<0.05) suggesting that epithelial dedifferentiation driven by loss of PTEN is SMAD3 dependent. These data are consistent with diminished expression of vimentin in (PTEN+SMAD3) shRNA cells relative

to (PTEN+con) shRNA cultures (Fig. 4C). HK-2 cells with dual PTEN and SMAD3 silencing are more proliferative both at day 3 and day 5 compared to (PTEN+con) shRNA cells (Fig. 4F; $P<0.05$ and $P<0.01$ respectively) confirming that PTEN-loss induced epithelial growth inhibition is orchestrated, at least in part, by SMAD3. Furthermore, elongated morphology and proliferative arrest characteristic of the PTEN inhibitor VO-treated HK-2 cells is effectively blocked by preincubation with the SMAD3 inhibitor, SIS3 (Fig. 4G) further placing SMAD3 downstream of PTEN inhibition in promoting phenotypic transitions in renal epithelial cells. pAkt, pSMAD3 and fibronectin expression evident in PTEN shRNA expressing cells were significantly diminished by the pre-incubation of an Akt inhibitor, MK-2206 (Fig. 4H). Similarly, growth inhibition observed in PTEN depleted HK-2 cells is also relieved by MK-2206 treatment (Fig 4I), suggestive of an upstream role of PTEN loss mediated Akt activation in pSMAD3 dependent fibrotic responses.

Involvement of p53 in PTEN-mediated fibrotic responses

p53, an established regulator of cell cycle arrest, mediates the progression of kidney injury to fibrosis (24,26). PTEN loss correlated with increased p53 activation and expression suggestive of a functional involvement between PTEN and p53 in renal disease progression (Fig. 1 & Fig. S1). PTEN depletion in HK-2 renal epithelial cells resulted in > 4-fold increase in $p53^{Ser15}$ phosphorylation compared to control shRNA cells (Fig. 5A&B; $P<0.05$). p53 and SMAD3 interactions and complex formation were previously implicated as critical for TGF–β1 mediated PAI-1 promoter activation (28). Immuno-precipitation analysis demonstrated increased interactions between endogenous pSMAD2/3 and p53 (Fig. 5C; left panel) and simultaneous activation of both p53 and pSMAD2/3 was evident in input lysates (Fig. 5C; right panel) in PTEN-depleted epithelial cells relative to con shRNA cells. To evaluate p53 as a downstream effector of PTEN, early passage PTEN stably silenced HK-2 cells were virally transduced with p53 or control shRNA expression constructs. Immuno-blot analysis confirmed silencing of both PTEN and p53 expression [termed (PTEN+p53) shRNA cells] while PTEN shRNA cells transduced with control vector [(PTEN+con) shRNA] retained p53 expression (Fig. 5D). Cell density evaluations of (PTEN +con) and (PTEN+p53) shRNA cells confirmed the role of p53 activation in epithelial proliferative arrest imposed by PTEN absence as HK-2 cells with dual silencing of PTEN and p53 cells reached significantly higher cell numbers compared to (PTEN+con) shRNA cultures (Fig. 5E; $P<0.001$). Moreover, the VO-mediated decrease in cell number in HK-2 cells can be blocked by pre-incubation with the p53 inhibitor Pifithrin-α prior to adding VO, as assessed by Crystal Violet staining (Fig. 5F) and cell count analysis (Fig 5G), further suggesting that p53 is a downstream target of PTEN loss or inactivation.

PAI-1 induction is causatively linked to epithelial growth inhibition orchestrated by PTEN loss

Elevated PAI-1 levels contribute to kidney disease progression as mice with PAI-1 deficiency are largely protected from injury induced (e.g., UUO) renal fibrosis (19,27). Loss of PTEN expression correlated with increased PAI-1 levels in the obstructed kidney (Fig. 1) and PTEN knockdown in HK-2 cells promoted PAI-1 expression (Fig. 3). The role of PAI-1 in the context of PTEN loss initiated epithelial dysfunction (i.e., growth arrest, fibrotic factor secretion), however, is unknown. Silencing of PAI-1 expression in HK-2 cultures by PTEN

gene knockdown [termed (PTEN+PAI-1) shRNA] exhibited higher population densities relative to PTEN-deficient cells infected with the control vector [(PTEN+con) shRNA] as assessed by Crystal Violet staining (Fig. S2A) and cell count after 3 days (Fig. S2B; $P < 0.05$). Increased density evident in (PTEN+PAI-1) shRNA cultures is comparable to that of cells with stable silencing of both p53 and PTEN expression (Fig. S2A & Fig. 5E). Furthermore, PCNA expression is significantly higher in both (PTEN+PAI-1) shRNA and (PTEN+p53) shRNA-expressing HK-2 cells compared with equally seeded (PTEN+con) shRNA cultures while the growth arrest marker p21 expression showed the opposite pattern (Fig. S2C), demonstrating that depletion of p53 or PAI-1 levels leads to a by-pass of cell growth inhibition triggered by PTEN loss in HK-2 cells. Elevated PAI-1 expression evident in (PTEN+con) shRNA cultures is decreased (>50%) in (PTEN+p53) shRNA cultures suggesting a role for p53 in mediating fibrotic gene induction (Fig. S2C&D; $P<0.05$). Moreover, (PTEN+Con) shRNA cells are more susceptible to cell death due to nutrient deprivation (induced by serum withdrawal at high confluence) than (PTEN+p53) shRNA (Fig. S2E) and (PTEN+PAI-1) shRNA (Fig. S2F) cells, suggesting that p53 and PAI-1 activation downstream of PTEN orchestrates the epithelial injury response to cellular stress.

PTEN loss cooperates with TGF-β1 in promoting fibrotic gene expression and epithelial cell apoptosis

Concurrent loss of tubulo-interstitial PTEN expression and elevated pSMAD3 signaling in the obstructed kidney necessitated an investigation of potential cross-talk between the TGF-β1 pathway and PTEN in renal epithelial cells and fibroblasts (Fig. 1). Indeed, TGF-β1-induced fibronectin (Fig. S3A&B; $P<0.01$), PAI-1 (Fig. S3A&C; $P<0.05$) synthesis and pSMAD3 phosphorylation (Fig. S3A&D; $p<0.05$), CTGF and vimentin (Fig. S3A) in mock-transduced (con shRNA) cultures is further enhanced in HK-2 cells with stable PTEN knockdown. Similarly, PTEN inactivation by VO pretreatment prior to TGF-β1 stimulation further enhanced PAI-1 and α-SMA expression relative to TGF-β1 treated NRK-49F renal fibroblasts (Fig. S3E). Since TGF-β1 induced PAI-1 expression is dependent on transcription (28), we determined whether PTEN and TGF-β1 cross-talk occurs at the level of PAI-1 transcription as well. Mv1Lu cells stably expressing an 800 bp PAI-1 promoter linked to a luciferase reporter (Mv1Lu-800bp-Luc cells) were pretreated with VO to inactivate PTEN prior to TGF-β1 addition. TGF-β1-mediated luciferase reporter activation was further enhanced by PTEN inactivation (Fig. S3F; $P<0.001$). Moreover, modest overexpression of PTEN (~2.5-fold) by viral transduction significantly suppressed TGF-β1 induced PAI-1 expression and SMAD3 activation compared to HK-2 cells expressing the control vector (Fig. S3G), suggesting that PTEN could negatively impact TGF-β1/SMAD3 driven target gene expression.

Tubular cell death and growth arrest are hallmarks of renal injury and significant contributors to disease progression (4–6). TGF-β1, a potent growth inhibitor in certain circumstances, could also promote apoptosis although the associated molecular mechanisms in renal pathology are not well understood. TGF-β1 also potentiates cell death induced by staurosporine in renal epithelial cells (32). To evaluate long-term effects of TGF-β1 stimulation in PTEN-deficient epithelial cells, confluent PTEN- or con shRNA-expressing HK-2 cells were maintained with or without TGF-β1 stimulation for 5–7 days. TGF-β1

treatment or PTEN loss resulted in modest cell death or a reduction in attached cells at days 5–7 (Fig. S4A–C). TGF-β1-treated PTEN shRNA cultures, in sharp contrast, underwent massive cell death with complete lifting of the cell monolayer at day 7 (Supplementary Fig. S4A&B; $P<0.001$); phase contrast microscopy at day 5 confirms higher cell death rates readily evident in these cultures (Fig. S4C) as well as increased cleaved caspase 3 expression (Fig. S4D), suggesting cooperativity between TGF-β1 treatment and PTEN loss in promoting apoptosis. Comparison of similarly confluent HK-2 cells with dual PTEN+p53 depletion to (PTEN+con) shRNA cultures stimulated with TGF-β1 suggests that PTEN +TGF-β1-initiated cell death is mediated, at least in part, by p53 as (PTEN+p53) shRNA cultures are protected from apoptosis, unlike (PTEN+con) shRNA cultures which underwent cell death in response to cytokine stimulation (Fig. S4E&F).

Discussion

Using UUO-, AAN- and STZ-induced kidney injury as mouse models, this study demonstrates that tubulo-interstitial expression of PTEN is dramatically decreased in the diseased kidney relative to the respective control kidneys. Normal kidneys exhibit significant tubular expression of PTEN supporting the contention that PTEN is a marker of epithelial integrity and differentiation. Stable silencing of PTEN in renal tubular epithelial cells promotes not only cellular dedifferentiation (marked by the acquisition of a fibroblastoid appearance and the induction of mesenchymal genes including vimentin and α–SMA) but also results in G1 cell cycle arrest and induction of fibrosis-causative factors (e.g., CTGF, fibronectin and PAI-1), leading to maladaptive tubular repair. Accordingly, loss of PTEN expression in the damaged tubules correlated with increased fibrosis in the obstructed kidney.

The present study identified novel causative roles for SMAD3 and p53 activation (in addition to Akt involvement) downstream of PTEN in promoting tubular dysfunction via SMAD3/p53-dependent secretion of fibrotic factors and the induction of epithelial proliferative arrest as well as SMAD3-dependent epithelial dedifferentiation. The loss of PTEN expression, in fact, correlated with increased p-p53^{Ser15} and pSMAD3 levels in the fibrotic UUO kidney. These observations have certain parallels to the molecular events of prostate cancer development where cancer initiation by PTEN ablation in mouse prostate is associated with SMAD2/3 activation and increased p53 expression with subsequent establishment of a senescence barrier against tumourigenesis (33,34). PTEN loss in other neoplasms, however, promotes AKT-mediated cancer growth suggesting that downstream effectors such p53 activation critically regulates eventual cell growth/inhibitory and fibrotic phenotype.

Our study also demonstrates that PAI-1 induction by PTEN depletion is linked to proliferative arrest in HK-2 cells highlighting a novel role for this serine protease inhibitor in renal tubular growth restriction. Expression of PAI-1 in this scenario is mediated by SMAD3/ p53-driven mechanisms, confirming the upstream role of these factors in promoting PAI-1-dependent proliferative arrest. These findings are in agreement with prior reports that (a) PAI-1 mediates TGF-β1-driven proliferative arrest in human keratinocytes (35), (b) SMAD3 and p53 are required for PAI-1 transcription by TGF-β1 in renal epithelial

cells (28), (c) there is extensive tubular co-localization of PAI-1, SMAD3 and p53 expression in the damaged UUO kidneys (27) and (d) mice with transgenic PAI-1 overexpression subjected to UUO have exacerbated tubular/renal injury and fibrosis compared to normal mice (36). The precise mechanism by which PAI-1 regulates cell cycle progression is currently under investigation.

PTEN loss, moreover, leads to hyper-induced expression of certain TGF-β1 target genes, including fibronectin, CTGF, PAI-1 and vimentin in HK-2 cells. Cooperation between TGF-β1 and PTEN is also evident in tubular epithelial apoptosis. PTEN-depleted HK-2 cells, but not mock-transduced control cultures, subjected to prolonged TGF-β1 exposure underwent extensive cell death via p53-associated mechanisms. This suggests that loss of tubular PTEN expression in the context of elevated TGF-β1/SMAD signaling, as evident during kidney fibrosis (Fig. 1) could be causatively linked to nephron loss and excess extracellular matrix remodeling (Fig. 6).

The precise mechanisms of loss of PTEN expression during renal injury are not clear although TGF-β1-induced micro-RNAs including mir-192 suppressed PTEN levels during diabetic renal injury leading to podocyte hypertrophy (16) while mir-21-targeted PTEN expression promoted plasticity in epithelial cells (37). These findings are consistent with our observations that PTEN deregulation occurs at the level of post-transcription/translation as PTEN transcript levels between contralateral and UUO kidneys are statistically insignificant (Fig. S1).

Collectively, this study shows that PTEN loss in tubular cells initiated a series of events resulting in epithelial dedifferentiation, expression of a subset of fibrotic factors and growth arrest while PTEN inactivation promotes a proliferative phenotype in renal fibroblasts. These findings also suggest that simultaneous targeting of the p53 and SMAD3 pathway may be an attractive strategy to restrict the development of PTEN loss-initiated tubular dysfunction and progression of renal fibrotic lesions.

Supplementary Material

Refer to Web version on PubMed Central for supplementary material.

Acknowledgements

Supported by NIH Grant GM057242 to PJH.

Abbreviations

PTEN	Phosphate Tensin Homologue on Chomosome 10
UUO	unilateral ureteral obstruction
AAN	aristolochic acid nephropathy
STZ	streptozotocin mediated injury
TGF-β1	transforming growth factor-β1

ALK5	TGF-β type I receptor kinase
TGF-β1-RI/II	transforming growth factor-β1-receptor I/II
α-SMA	α-smooth muscle actin
CKD	chronic kidney disease
COX-2	cyclooxygenase-2
CTGF	connective tissue growth factor
DAB	diaminobenzidine
DMEM	Dulbecco's modified Eagle's Medium
FBS	fetal bovine serum
GAPDH	glyceraldehyde 3-phosphate dehydrogenase
HK-2	human proximal tubular cells
NRK-49F	normal rat kidney fibroblasts
PAI-1	plasminogen activator inhibitor-1
PBS	phosphate-buffered saline
PCNA	proliferating cell nuclear antigen
ROS	reactive oxygen species
SDS-PAGE	sodium dodecyl sulfate polyacrylamide gel electrophoresis
VO	VO-OHpic trihydrate
CTGF	connective tissue growth factor

References

1. Jha V, Garcia-Garcia G, Iseki K, et al. Chronic kidney disease: global dimension and perspectives. Lancet. 2013; 382(9888):260–272. [PubMed: 23727169]
2. Perico N, Remuzzi G. Chronic kidney disease: a research and public health priority. Nephrol Dial Transplant. 2012; 27(Supple 3):iii19–iii26. [PubMed: 22764188]
3. Couser WG, Remuzzi G, Mendis S, et al. The contribution of chronic kidney disease to the global burden of major noncommunicable diseases. Kidney Int. 2011; 12:1258–1270. [PubMed: 21993585]
4. Strutz F, Neilson EG. New insights into mechanisms of fibrosis in immune renal injury. Springer Semin Immunopath. 2003; 24:459–476.
5. Eddy AA. Progression of chronic kidney disease. Adv Chronic Kidney Dis. 2005; 12:353–365. [PubMed: 16198274]
6. Yang L, Humphreys BD, Bonventre JV. Pathophysiology of acute kidney injury to chronic kidney disease: maladaptive repair. Contrib Nephrol. 2011; 174:149–155. [PubMed: 21921619]
7. Bottinger EP, Bitzer M. TGF-β signaling in renal disease. J Am Soc Nephrol. 2002; 13:2600–2610. [PubMed: 12239251]
8. Rüster C, Wolf G. Angiotensin II as a morphogenic cytokine stimulating renal fibrogenesis. J Am Soc Nephrol. 2011; 22:1189–1199. [PubMed: 21719784]
9. Friedman SL, Sheppard D, Duffield JS, et al. Therapy for fibrotic diseases: nearing the starting line. Sci Transl Med. 2013; 5(167):167sr.

10. Shi Y, Paluch BE, Wang X, et al. PTEN at a glance. J Cell Sci. 2012; 125:4687–4692. [PubMed: 23223894]
11. Song MS, Salmena L, Pandolfi PP. The functions and regulation of the PTEN tumour suppressor. Nat Rev Mol Cell Biol. 2012; 13:283–296. [PubMed: 22473468]
12. White ES, Atrasz RG, Hu B, et al. Negative regulation of myofibroblast differentiation by PTEN (Phosphatase and Tensin Homolog Deleted on chromosome 10). Am J Respir Crit Care Med. 2006; 173:112–121. [PubMed: 16179636]
13. Miyoshi K, Yanagi S, Kawahara K, et al. Epithelial Pten controls acute lung injury and fibrosis by regulating alveolar epithelial cell integrity. Am J Respir Crit Care Med. 2013; 187:262–275. [PubMed: 23239155]
14. López-Novoa JM, Nieto MA. Inflammation and EMT: an alliance towards organ fibrosis and cancer progression. EMBO Mol Med. 2009; 1(6–7):303–314. [PubMed: 20049734]
15. Parapuram SK, Shi-wen X, Elliott C, et al. Loss of PTEN expression by dermal fibroblasts causes skin fibrosis. J Invest Dermatol. 2011; 131:1996–2003. [PubMed: 21654839]
16. Kato M, Putta S, Wang M, et al. TGF-beta activates Akt kinase through a microRNA-dependent amplifying circuit targeting PTEN. Nat Cell Biol. 2009; 11:881–889. [PubMed: 19543271]
17. Lan Geng H, Polichnowski AJ, Singha PK, et al. PTEN loss defines a TGF-β-induced tubule phenotype of failed differentiation and JNK signaling during renal fibrosis. Am J Physiol Renal Physiol. 2012; 302:F1210–F1223. [PubMed: 22301622]
18. Mahimainathan L, Das F, Venkatesan B, et al. Mesangial cell hypertrophy by high glucose is mediated by downregulation of the tumor suppressor PTEN. Diabetes. 2006; 55:2115–2125. [PubMed: 16804083]
19. Eddy AA, Fogo AB. Plasminogen activator inhibitor-1 in chronic kidney disease: evidence and mechanisms of action. J Am Soc Nephrol. 2006; 17:2999–3012. [PubMed: 17035608]
20. Samarakoon R, Overstreet JM, Higgins SP, et al. TGF-β1→SMAD/p53/USF2→PAI-1 transcriptional axis in UUO-induced renal fibrosis. Cell Tissue Research. 2012; 347:117–128. [PubMed: 21638209]
21. Samarakoon R, Overstreet JM, Higgins PJ. TGF-β signaling in tissue fibrosis; redox controls, target genes and therapeutic opportunities. Cell Signal. 2012; 25:264–268. [PubMed: 23063463]
22. Shi-Wen X, Leask A, Abraham D. Regulation and function of connective tissue growth factor/CCN2 in tissue repair, scarring and fibrosis. Cytokine Growth Factor Rev. 2008; 19:133–144. [PubMed: 18358427]
23. Massagué J. TGFβ signalling in context. Nat Rev Mol Cell Biol. 2012; 13:616–630. [PubMed: 22992590]
24. Yang L, Besschetnova TY, Brooks CR, et al. Epithelial cell cycle arrest in G2/M mediates kidney fibrosis after injury. Nat Med. 2010; 16:535–543. [PubMed: 20436483]
25. Zhou L, Fu P, Huang XR, et al. Activation of p53 promotes renal injury in acute aristolochic acid nephropathy. J Am Soc Nephrol. 2010; 21:31–41. [PubMed: 19892935]
26. Ying Y, Kim J, Westphal SN, et al. Targeted Deletion of p53 in the Proximal Tubule Prevents Ischemic Renal Injury. J Am Soc Nephrol. 2014 May 22. pii: ASN.2013121270. [Epub ahead of print].
27. Samarakoon R, Dobberfuhl AD, Cooley C, et al. Induction of Renal Fibrotic Genes by TGF-β1 Requires EGFR Activation, p53 and Reactive Oxygen Species. Cell Signal. 2013; 25:2198–2209. [PubMed: 23872073]
28. Overstreet JM, Samarakoon R, Higgins PJ. Redox control of p53 in the transcriptional regulation of TGF-β target genes through SMAD cooperativity. Cell Signal. 2014; 26:1427–1436. [PubMed: 24613410]
29. Falke LL, Dendooven A, Leeuwis JW, et al. Hemizygous deletion of CTGF/CCN2 does not suffice to prevent fibrosis of the severely injured kidney. Matrix Biol. 2012; 31:421–431. [PubMed: 23199377]
30. Chevalier RL, Forbes MS, Thornhill BA. Ureteral obstruction as a model of renal interstitial fibrosis and obstructive nephropathy. Kidney Int. 2009; 75:1145–1152. [PubMed: 19340094]

31. Gökmen MR, Cosyns JP, Arlt VM, et al. The epidemiology, diagnosis, and management of aristolochic acid nephropathy: a narrative review. Ann Intern Med. 2013; 158:469–477. [PubMed: 23552405]

32. Dai C, Yang J, Liu Y. Transforming growth factor-beta1 potentiates renal tubular epithelial cell death by a mechanism independent of Smad signaling. J Biol Chem. 2003; 14:12537–12545. [PubMed: 12560323]

33. Chen Z, Trotman LC, Shaffer D, et al. Crucial role of p53-dependent cellular senescence in suppression of Pten-deficient tumorigenesis. Nature. 2005; 436:725–730. [PubMed: 16079851]

34. Ding Z, Wu CJ, Chu GC, et al. SMAD4-dependent barrier constrains prostate cancer growth and metastatic progression. Nature. 2011; 470:269–273. [PubMed: 21289624]

35. Kortlever RM, Nijwening JH, Bernards R. Transforming growth factor-beta requires its target plasminogen activator inhibitor-1 for cytostatic activity. J Biol Chem. 2008; 283:24308–24313. [PubMed: 18614541]

36. Matsuo S, López-Guisa JM, Cai X, et al. Multifunctionality of PAI-1 in fibrogenesis: evidence from obstructive nephropathy in PAI-1-overexpressing mice. Kidney Int. 2005; 67:2221. [PubMed: 15882265]

37. Zhou Y, Xiong M, Fang L, et al. miR-21 containing microvesicles from injured tubular epithelial cells promote tubular phenotype transition by targeting PTEN protein. Am J Pathol. 2013; 183:1183–1196. [PubMed: 23978520]

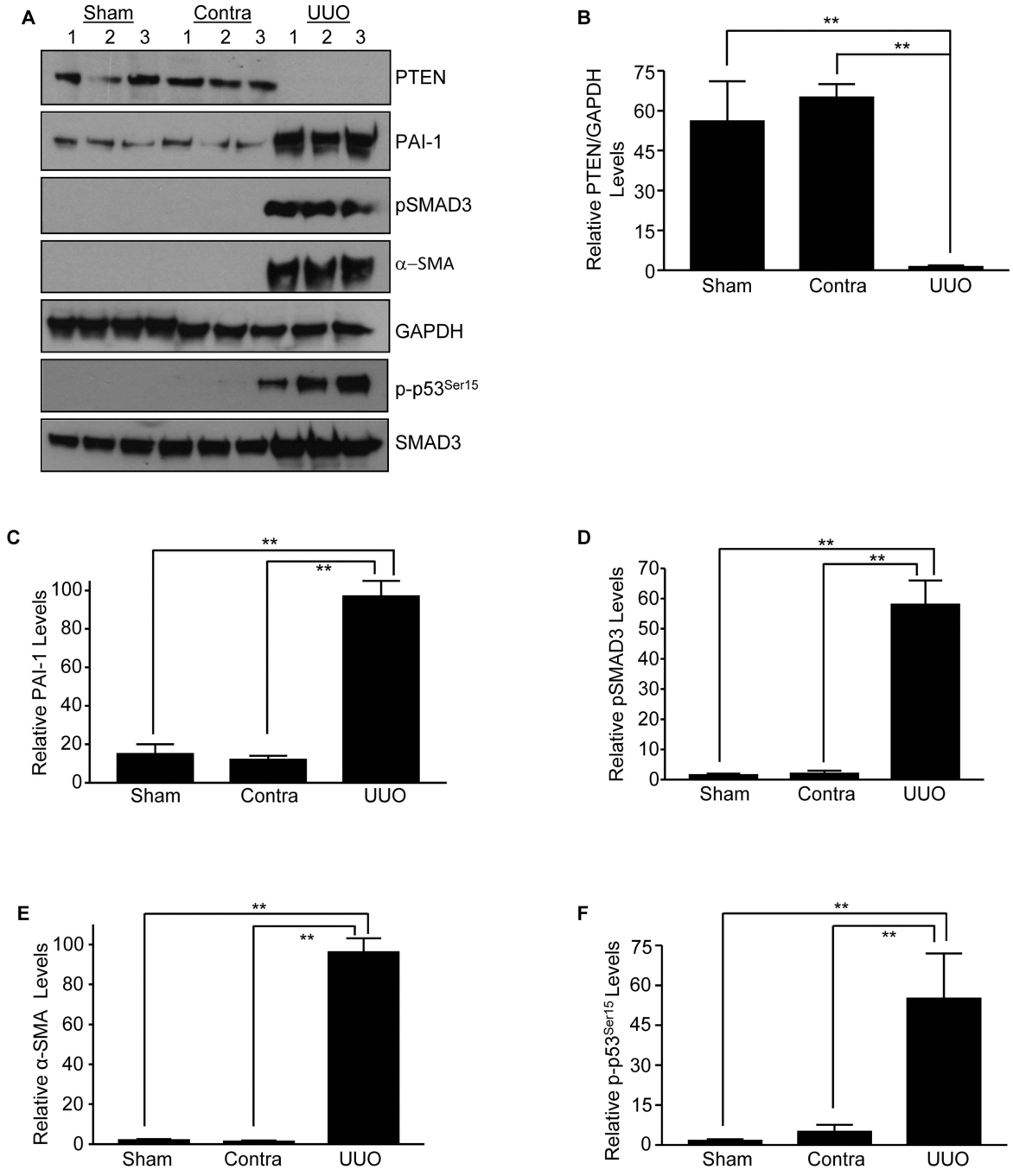

Figure 1. Correlation of loss of PTEN expression with renal fibrosis induced by ureteral ligation

Western blot analysis for PTEN (**A&B**), PAI-1 (**A&C**) pSMAD3 (**A&D**), α-SMA (**A&E**), p-p53^{Ser15} (**A&F**) SMAD3 and GAPDH (a loading marker) expression levels in sham, contralateral (Contra) and obstructed (UUO) mouse kidneys at day 14 (n=3–5 for each condition). Histograms (mean±s.d) (**B–F**) depict relative expression of the markers indicated. P-values: *$P < 0.05$ and **$P < 0.01$ as indicated between UUO and contralateral or sham controls.

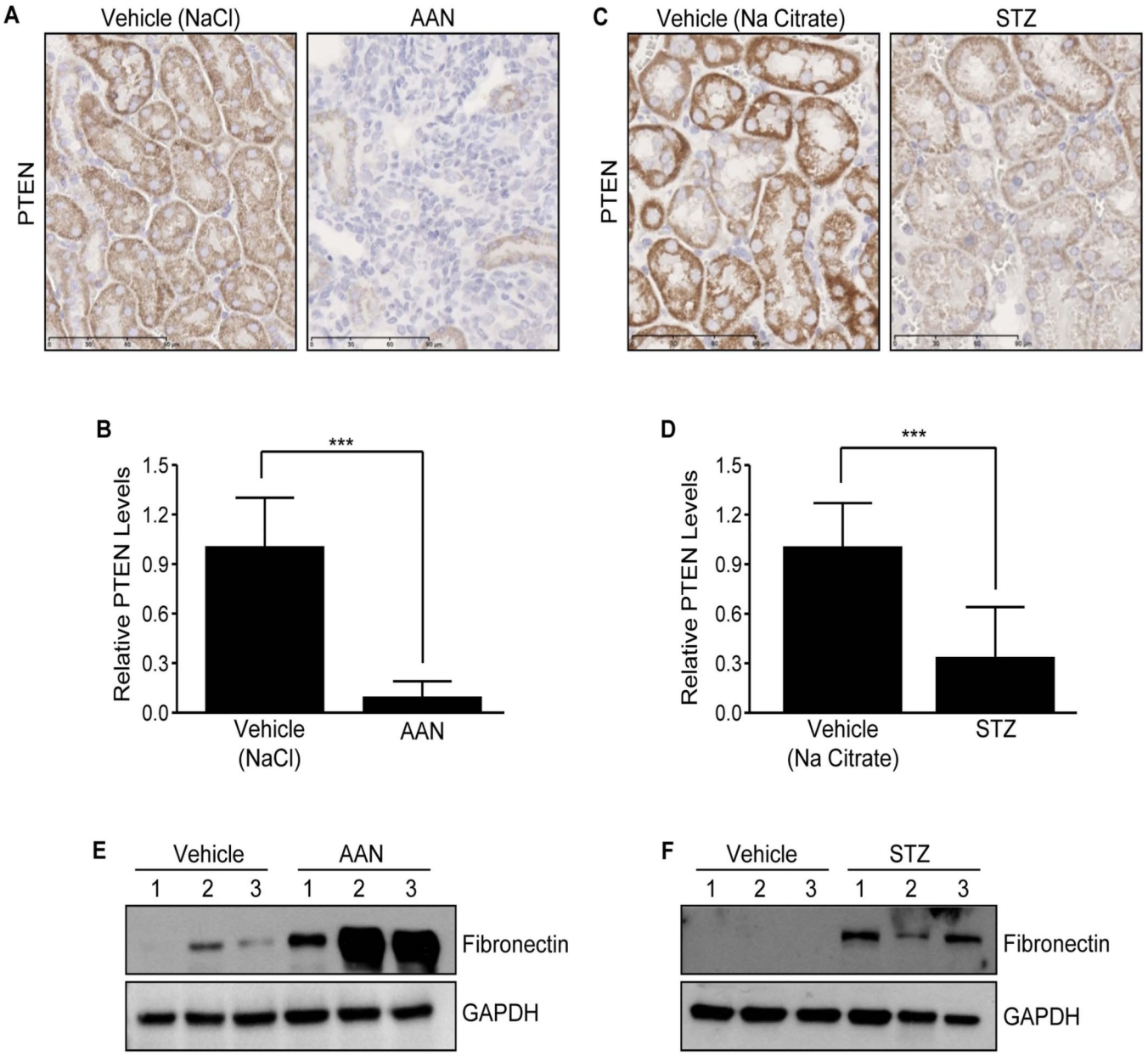

Figure 2. Tubulo-interstitial loss of PTEN in aristolochic acid nephopathy (AAN) and streptozotocin-induced nephropathy (STZ)

Immunostaining of kidneys from mice treated with aristolochic acid (AA; 5 mg/kg for 25 days) or NaCl vehicle (**A**) and renal sections from mice injected with STZ or control Na citrate buffer with anti-rabbit antibodies to PTEN (**C**). Histograms illustrate relative DAB staining indicative of PTEN levels in the AAN and STZ kidneys (mean±s.d) in **B** and **D**, respectively; DAB intensities for respective vehicle-treated kidneys (controls) were set as 1. ***$P < 0.001$ versus NaCl vehicle (for AAN), ***$P < 0.001$ versus Na citrate buffer (for STZ). IHC was repeated multiple times in different mice and representative images were shown. Scale bar= 90μM. Relative assessments NaCl vehicle and AAN-treated and Na

citrate vehicle and STZ-treated kidney lysates for of fibronectin and GAPDH expression in shown in **E & F** respectively. N=3 animals for AAN as well as for STZ experiments.

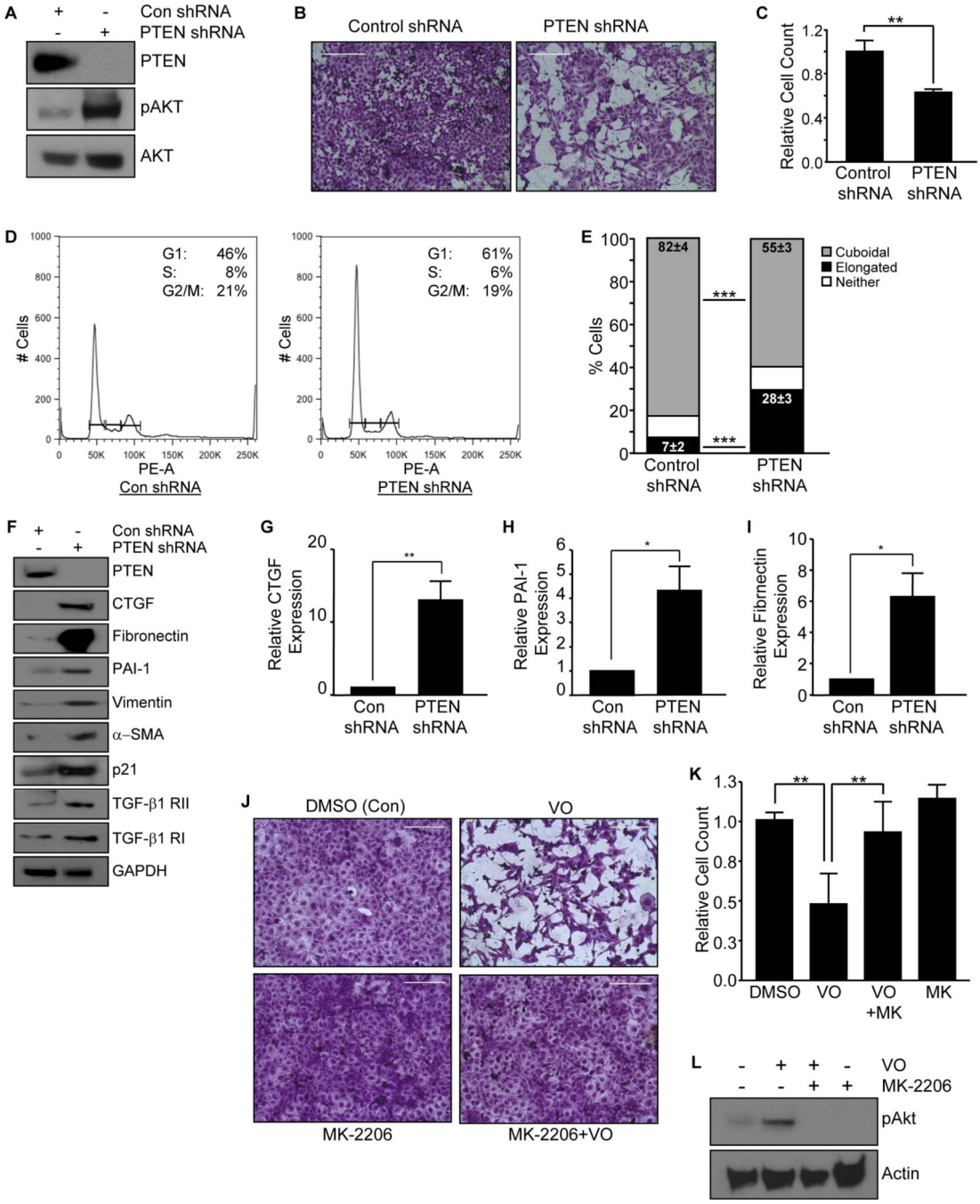

Figure 3. Gene silencing and inhibition of PTEN expression in HK-2 tubular epithelial cells promotes G1 arrest, morphological transition and profibrotic gene expression

PTEN and control (Con) shRNA expressing cultures were assessed for PTEN, pAkt and total Akt expression levels by western analysis (**A**). Crystal Violet staining of equally-seeded HK-2 cells with stable PTEN knockdown or control shRNA in complete media for 3–5 days (**B**). Cell number for each experimental condition was determined in triplicate (mean±s.d) and is shown in (**C**), setting control shRNA as 1. $^{**}P < 0.01$. Propidium iodide staining followed by flow analysis of PTEN and Con shRNA expressing cells grown in

complete media for 2–3 days was utilized to assess cell cycle distribution (**D**). Insets in each histogram highlight the percentages of G1, S, and G2/M phase cells for Con shRNA or PTEN-knockdown cultures. The histogram illustrates the relative changes in morphology (e.g., elongated [i.e., fibroblastoid], cuboidal or neither) in PTEN or control (Con) shRNA expressing cells after 3–5 days as a percentage of total population (mean±s.d) (**E**). ***P < 0.001 for both elongated and cuboidal morphology changes. Sub-confluent Con and PTEN shRNA expressing cell cultures were maintained in low serum (0.1%) for 3–5 days and extracted lysates analysed by western blotting with antibodies to CTGF (**F&G**), PAI-1 (**F&H**), fibronectin (**F&I**), α–SMA, vimentin, p21, TGF-β1 RI and RII and GAPDH (a loading control) (**F**). The histogram (mean±s.d) depicts a summary of three independent assessments of the relative expression of CTGF (**F**), PAI-1 (**H**) and fibronectin (**I**) in PTEN depleted cells setting the levels of control shRNA cells as 1. *P < 0.05, **P < 0.01. VO-OHpic trihydrate (VO) treatment was utilized to inhibit PTEN expression in HK-2 cells. Crystal Violet staining of VO-treated (1μM for 48 hours) or DMSO control HK-2 cells with or without Akt inhibitor pretreatment (**J**). Scale= 200μM. Cell count analysis for each experimental condition in triplicate (mean±s.d) is shown in (**K**) setting DMSO control as 1. *P < 0.05, **P < 0.01, as indicated between groups. Western analysis of DMSO/control, Akt inhibitor-MK-2206 (1nM)-, VO- and MK-2206+VO-treated cultures for pAKT and actin expression is presented in (**L**). MK=MK-2206.

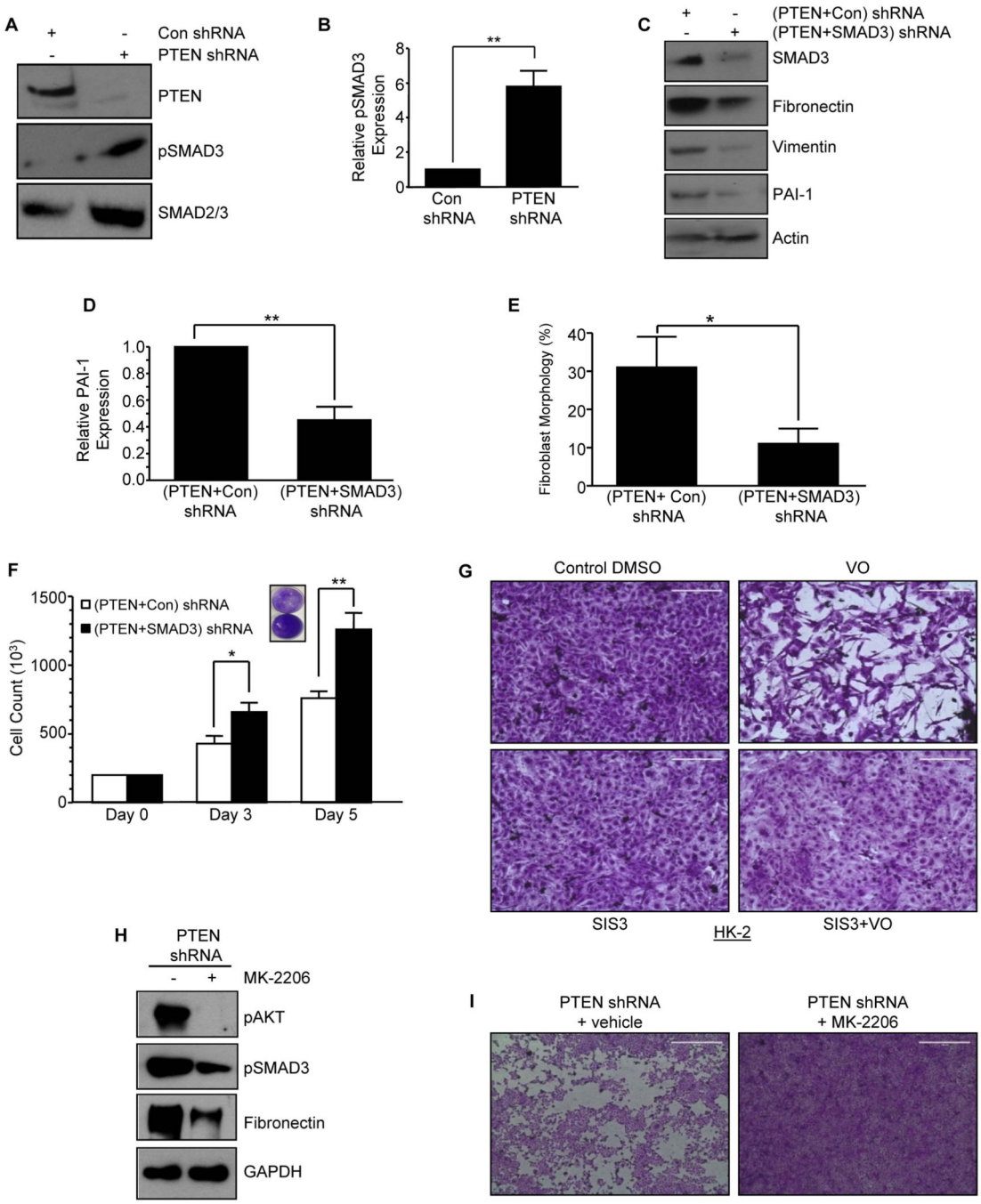

Figure 4. SMAD3 activation in response to PTEN loss in tubular cells promotes growth inhibition and fibrotic markers

Control and PTEN shRNA expressing cells were serum deprived for 2–3 days and lysate extracts subjected to western analysis with PTEN, pSMAD3 and total SMAD3 antibodies (**A**). A summary of 3 independent experiments (mean±s.d) for relative pSMAD3 levels in PTEN-depleted cultures relative to control shRNA (set as 1) is presented in the graph (**B**). $^{**}P < 0.01$. Early passage PTEN- depleted HK-2 cultures stably expressing SMAD3 shRNA [(PTEN+SMAD3) shRNA)] or control shRNA [(PTEN+Con) shRNA)] were serum-

deprived for 3 days. Extracts of (PTEN+Con) shRNA or (PTEN+SMAD3) shRNA cells were western blotted with antibodies to SMAD3, fibronectin, PAI-1 (**C&D**), vimentin or GAPDH (**C**). The histogram (**E**) depicts percentage of cells (mean±s.d) with fibroblast/elongated morphology for (PTEN+ Con) shRNA and (PTEN+SMAD3) shRNA cultures as determined by triplicate assessments for each group. **P* < 0.05. Equally seeded (20,000 cells) (PTEN+Con) shRNA or (PTEN+SMAD3) shRNA expressing cultures were grown for 3–5 days; the histogram is a plot of triplicate cell counts (mean±s.d) for each condition (**F)**. **P* < 0.05 versus control shRNA at day 3, ***P* < 0.01 versus control shRNA at day 5. Inset in (**F)** is the Crystal Violet images of indicated cultures. Semi-confluent (80%) HK-2 cells were treated with the PTEN inhibitor VO (1 μM; 24–48hrs) or DMSO control with or without preincubation with the SMAD3 inhibitor SIS3 (5μM) and stained with Crystal Violet (**G**). Lysate extracts of semi-confluent PTEN shRNA expressing cells treated with MK-2206 or vehicle for 3 days were immuno-blotted for pAkt, pSMAD3, fibronectin and GAPDH expression (**H**). Crystal violet images of similarly confluent PTEN depleted cells treated with DMSO vehicle or MK-2206 cells for 3 days **(I**). Scale=1000μM.

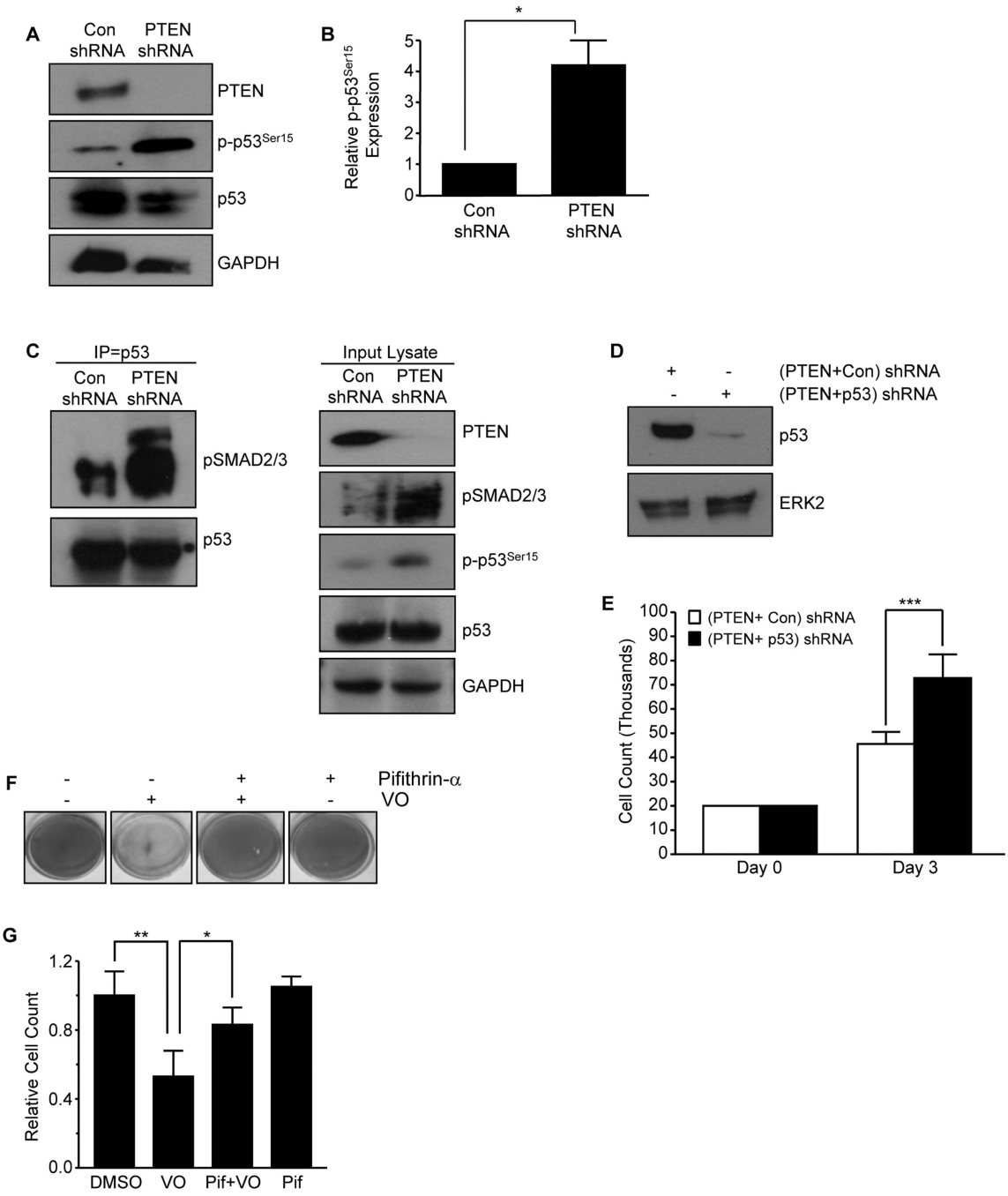

Figure 5. p53 activation upon loss of PTEN contributes to defective epithelial growth and fibrotic properties

Confluent PTEN or Con shRNA stably expressing cells were serum-deprived for 2–3 days and lysates immuno-blotted with PTEN, p-p53^{Ser15}, p53 and GAPDH antibodies **(A)**. The histogram (mean±s.d) in (**B)** is a summary of 3 independent experiments to assess p-p53^{Ser15} levels in PTEN depleted cells relative to control (Con) shRNA cultures (set as 1). *$P < 0.05$. Equal lysate fractions derived from an identical set of control and PTEN shRNA cultures were immuno-precipitated with a mouse anti-p53 antibody (2 μg) followed by

western analysis with rabbit anti-pSMAD2/3 or rabbit anti-p53 antibodies (**C**). Input lysates were western blotted for PTEN, pSMAD2/3, p-p53^{Ser15}, p53 or GAPDH (a loading marker) (**C**). Early passage PTEN shRNA cells were re-infected with p53 shRNA (termed PTEN +p53 shRNA) or control shRNA (termed PTEN+Con shRNA) constructs. (PTEN+Con) shRNA or (PTEN+p53) shRNA stably-expressing cells were serum deprived for 3 days and immuno-blotted for p53 or ERK2 (a loading marker) expression (**D**). Growth assessments for equally seeded (20,000 cells) (PTEN+Con) shRNA- or (PTEN+p53) shRNA cultures after 3 days; plot illustrates cell counts in triplicate cultures (mean±s.d) (**E**). ***$P < 0.001$ versus (PTEN+con) shRNA. Crystal Violet staining of confluent HK-2 cells pretreated with the p53 inhibitor Pifithrin-α (10 μM; 18 hrs) prior to stimulating with VO (1 μM) for 24–48 hours is shown in (**F**). Triplicate cell count analysis for each experimental condition (mean ±s.d) relative to control (set as 1) is expressed in the plot (**G**). *$P < 0.05$, **$P < 0.01$.

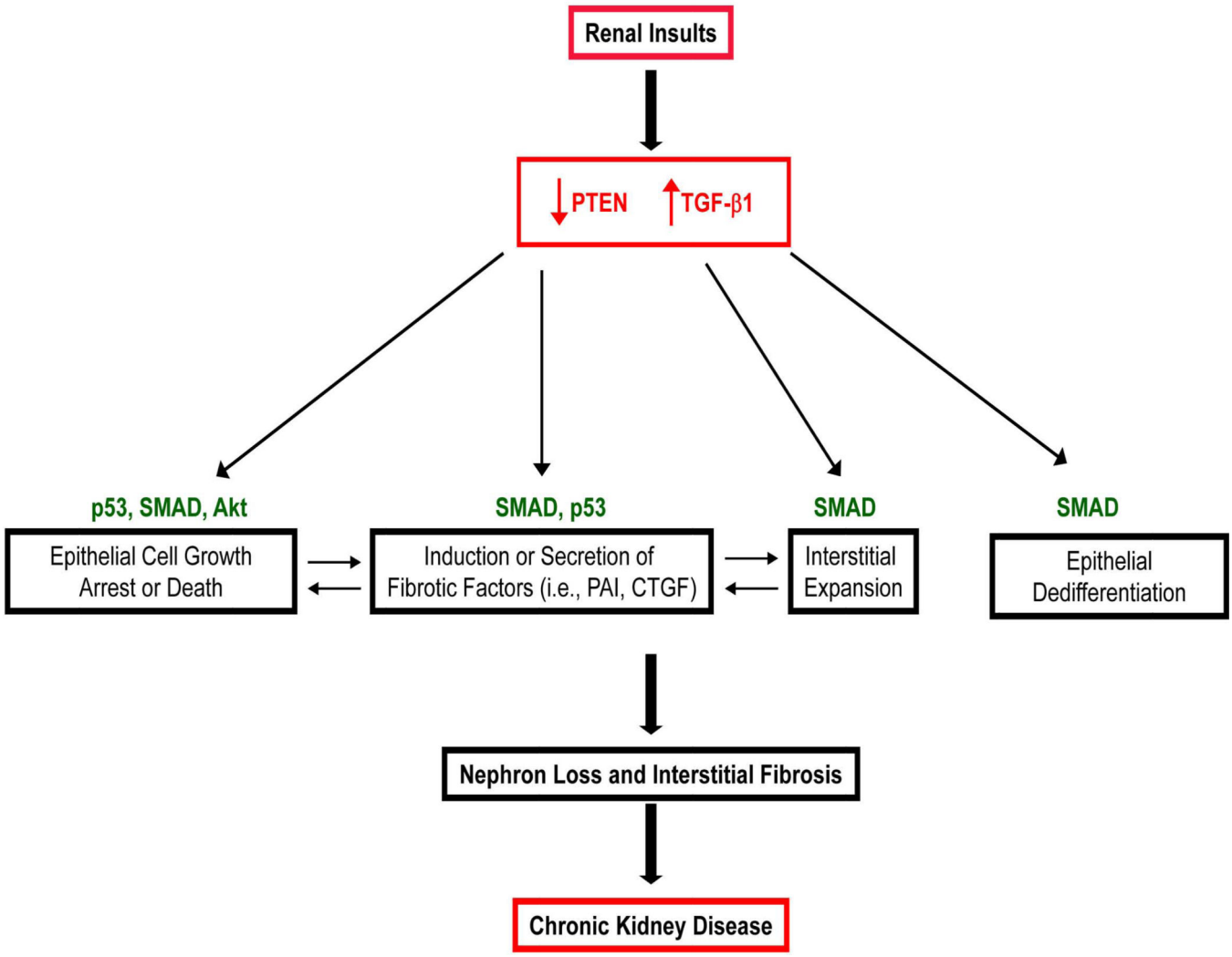

Figure 6. Model for PTEN and TGF-β1 Mediated Cross-talk in Renal Fibrosis

PTEN loss initiates Akt, SMAD2/3 and p53 signaling impacting fibrotic gene expression, epithelial plasticity, epithelial cell growth arrest/death leading to tubular dysfunction and nephron loss and myofibroblast accumulation, which are common elements of fibrotic scarring and chronic kidney disease. In concert with TGF-β1, PTEN deficiency further promotes fibrotic factor induction and epithelial cell death.